Chlorine Radical-Initiated Atmospheric Oxidation of Imines: Implications for Structural Influence on the Nitrosamine Formation

Qian Xu[1], Fangfang Ma[1,2]*, Chang Liu[1], Qiaojing Zhao[1], Jingwen Chen[1], Hong-Bin Xie[1]*

[1]Key Laboratory of Industrial Ecology and Environmental Engineering (Ministry of Education), School of Environmental Science and Technology, Dalian University of Technology, Dalian 116024, China

[2]College of Resources and Environmental Engineering, Guizhou Provincial Key Laboratory for Prevention and Control of Emerging Contaminants, Guizhou University, Guiyang, 550025, PR China

Correspondence to: ffma@gzu.edu.cn *(Fangfang Ma) and* hbxie@dlut.edu.cn *(Hong-Bin Xie)*

Abstract. Chlorine radical (·Cl) initiated atmospheric oxidation of organic nitrogen compounds (ONCs) plays an important role in carcinogenic nitrosamines formation. Imines are important constituents of ONCs, primarily formed from the atmospheric oxidation of amines. However, ·Cl-initiated atmospheric oxidation of imines remains poorly understood. Here, we studied the reaction mechanisms and kinetics of ·Cl-initiated atmospheric oxidation for five representative imines (CH_2=NH, CH_3CH=NH, CH_3N=CH_2, $(CH_3)_2C$=NH, HN=$CHCH_2OH$) to elucidate their atmospheric fate and extend the limited available data of ONCs, thereby establishing a structure-activity relationship for the reactions. The calculated overall reaction rate constants (× 10^{-11} cm^3 $molecule^{-1}$ s^{-1}) of ·Cl + CH_2=NH, ·Cl + CH_3CH=NH, ·Cl + CH_3N=CH_2, ·Cl + $(CH_3)_2C$=NH, and ·Cl + HN=$CHCH_2OH$ are 4.5, 27.2, 7.32, 44.8 and 12.6, respectively, which are consistent with the available experimental values. Importantly, our results show that ·Cl-initiated reactions of the NH-containing imines mainly produce N-centered radicals. These N-centered radicals exhibit various fates under tropospheric conditions: mainly reacting with NO to form nitrosamines or with O_2 to form cyanide compounds, which differs substantially from the behavior of previously reported amines. The various fates of the N-centered radicals formed from imines originates from the difference in direct hydrogen abstraction reaction rate constants (k_{O2}) with O_2 and the reaction rate (k_{NO}) with NO, both of which are principally governed by the distinct molecular structure of N-centered radicals. The revealed reaction mechanism provides new insights into the atmospheric transformation and risks of imines, and enrich our understanding of ·Cl/ONCs chemistry.

1 Introduction

Chlorine radicals (·Cl) are key atmospheric oxidants that significantly impact air quality and radical budgets by oxidizing volatile organic compounds (VOCs), thereby contributing to the formation of O_3, ·OH and secondary organic aerosol (SOA), and consequent impacts on climate (Gunthe et al., 2021; Liu et al., 2024; Wang et al., 2019; Yi et al., 2023; Cao et al., 2024; Ma et al., 2025). Historically, ·Cl was considered to originate mainly from heterogeneous reactions on sea salt particles (Faxon and Allen, 2013). In recent years, diverse sources of ·Cl precursors have been identified in urban and suburban

environments, e.g., coal combustion, biomass burning, road salt application, chlorine-based fertilizers, and automotive braking processes (Li et al., 2020; Fu et al., 2018; Li et al., 2024; Yin et al., 2022; Thornton et al., 2010; Cooke et al., 2025; Chen et al., 2025). Daytime ·Cl concentrations have been reported to reach up to 10^6 molecule cm^{-3}, comparable to typical ·OH concentrations (Young et al., 2014; Li et al., 2025; Wang et al., 2023). Laboratory and theoretical studies have shown that ·Cl-initiated oxidation of VOCs proceeds 10-100 times faster than those initiated by ·OH (Edwards and Young, 2024). Moreover, ·Cl-initiated oxidation of VOCs often follows distinct pathways and produce products that differ significantly from those of ·OH-initiated reactions (Chen et al., 2025; Guo et al., 2020; Wang et al., 2022). For example, ·Cl-initiated oxidation of VOCs could yield chlorine-containing products, potentially altering their toxicity (Fu et al., 2024; Ding et al., 2021). Thus, ·Cl-initiated reactions represent a crucial role in governing the fate of VOCs and warrant careful consideration.

Organic nitrogen compounds (ONCs), a major subclass of VOCs, account for approximately 65% of VOCs and are commonly detected in the atmosphere (Abudumutailifu et al., 2024). ONCs play significant roles in the formation of particles and hazardous substances, such as hydrogen cyanide (HCN), nitrous oxide (N_2O), nitrosamines, and nitramines (Ning et al., 2022; Wang et al., 2023; Liu et al., 2021; Abudumutailifu et al., 2024; Sun et al., 2024; Elm et al., 2016). Imines ($R_1R_2C=NR_3$) comprise about 16% of atmospheric ONCs (Ditto et al., 2022), which originate from multiple sources, including combustion, motor vehicles, cleaning sports equipment and the atmospheric oxidation of amines, the latter being the primary one (Waterman and Hillhouse, 2008; Zhu et al., 2022; You et al., 2022; Onel et al., 2014). In urban areas, imines have been detected at ppt levels, comparable to typical concentrations of amines (Zhu et al., 2022). Given their abundance and their role as first-generation oxidation products of amines, elucidating the atmospheric reaction mechanisms of imines is essential for accurately assessing their environmental impacts.

To date, only limited studies have investigated the atmospheric chemistry of imines (Ali, 2020; Xu et al., 2024; Ali et al., 2016; Bunkan et al., 2014; Akbar Ali et al., 2018; Bunkan et al., 2022; Almeida and Kurtén, 2022; Ditto et al., 2020; Yao et al., 2016). Atmospheric oxidation by ·OH and ·Cl are important removal pathways for imines. Previous experimental and theoretical studies have primarily examined the reaction mechanism and kinetics of ·OH-initiated reactions with simple imines, such as methylimine ($CH_2=NH$) (Bunkan et al., 2014; Akbar Ali et al., 2018), N-methylmethylimine ($CH_3N=CH_2$) (Bunkan et al., 2022), and cyclic imine 1,2,3,6-tetrahydropyrazine (THPyz) (Almeida and Kurtén, 2022). These studies demonstrated that the substituents on the C=N bond profoundly influence the reactivity of imines, ultimately leading to varying atmospheric impacts. Nevertheless, no previous studies have addressed ·Cl-initiated reactions of imines. Since ·OH and ·Cl-initiated reactions of ONCs follow distinct mechanisms and yielding different products (Xie et al., 2015; Xue et al., 2022; Xie et al., 2014), the reactivity of imines toward ·Cl cannot be directly inferred from their ·OH chemistry.

Our previous studies demonstrated that ·Cl exhibits a particularly strong interaction with the $-NH_x$ group of ONCs, leading to the formation of N-centered radicals, which are recognized precursors of carcinogenic nitrosamines (Xie et al., 2017; Liu et al., 2019). Additionally, the yield of N-centered radicals is strongly dependent on the structure of ONCs. Given the electronic structures of imines, ·Cl-initiated atmospheric oxidation of imines has the potential to form N-centered radicals. However, the

nitrogen lone pair electrons of imines can be delocalized to some extent to their adjacent C=N bond, which tends to decrease its electron-donor ability compared with previously well-studied ONCs (Carey and Sundberg, 2007), which may alter the reaction mechanisms of ·Cl + imines reactions. Moreover, the subsequent reactions of N-centered radicals depended on their specific structures. Therefore, to broaden our comprehension of the atmospheric chemistry of imines and fully assess their environmental risks, it is essential to elucidate the reaction mechanism and kinetics of ·Cl + imines reactions.

In this study, the reaction mechanisms and kinetics of imines with ·Cl were investigated by selecting five simple imines {i.e., methanimine (CH_2=NH), ethanimine (CH_3CH=NH), N-methylmethanimine (CH_3N=CH_2), 2-propanimine ((CH_3)$_2$C=NH), and 2-iminoethanol (HN=$CHCH_2OH$)} as model compounds. A combination of quantum chemical calculations and kinetic modeling was employed to elucidate these reactions. The parent amines of all selected imines have been detected in the ambient atmosphere (Qiu and Zhang, 2013; Ge et al., 2011; Shen et al., 2023). For the imine radicals yielded in the initial reaction step, their subsequent reactions including isomerization/dissociation, and bimolecular reactions with key atmospheric oxidants (O_2 and NO) were investigated. These results provide valuable insights into the reaction mechanisms and kinetics of imines, thereby advancing our understanding of their atmospheric chemistry and ·Cl chemistry.

2 Computational Details

2.1 Global Minimum Search. The selected imines can exist in multiple distinct gas-phase configurations. To identify their global minima, a multi-step conformational sampling scheme was employed, following our earlier studies (Lu et al., 2024; Ma et al., 2019; Ma et al., 2023) To explore their conformational space, the gentor module within the Molclus program was initially used to form the range of conformations (Lu, 2025). The generated conformers were further optimized at the PM6 and MP2/6-31+G(3df,2p) level (Vereecken and Francisco, 2012). Single-point energy calculations were performed at the CCSD(T)/aug-cc-pVTZ level (Vereecken and Francisco, 2012). The structures with the lowest Gibbs free energy were identified as the global minima and served as the initial structures for investigating the reaction mechanisms and kinetics. The corresponding global minima of five imines are presented in Figure S1.

2.2 Electronic Structure Calculations. All electronic structure calculations were conducted with the Gaussian 09 program package (Frisch et al., 2009). For the ·Cl-initiated reactions of five imines, geometry optimizations and harmonic vibrational frequency calculations were performed at the MP2/6-31+G(3df,2p) level, followed by single-point energy evaluations at the CCSD(T)/aug-cc-pVTZ level. This is consistent with our previous work on ·Cl-initiated reactions of ONCs systems, where the combination of MP2 and CCSD(T) methods has proven to yield reliable energies (Ma et al., 2018). Considering the substantially increased computational cost for the subsequent reactions of the resulting imine radicals, we employed the M06-2X/6-31+G(d,p) level for geometry optimizations and frequency calculations (Zhao and Truhlar, 2008), followed by CCSD(T)/6-311+G(2df,2p) single-point energy evaluations (Pople et al., 1989). The M06-2X functional combined with CCSD(T) method has successfully been applied to predict radical + O_2/NO reactions (Fu et al., 2024). Intrinsic reaction

coordinate (IRC) calculations were used to confirm that each transition state correctly connects the relevant reactants and products at the respective optimization levels (Fukui, 1981). The isolated ·Cl was treated with a correction value of 0.8 kcal mol^{-1} to account for spin-orbit coupling effects (Ma et al., 2018). Natural bond orbital (NBO) analysis was conducted to characterize the atomic charges in the transition states of initial reaction (Reed et al., 1985). Unless otherwise specified, the following labels are used throughout the manuscript: 'reactants' (R), 'pre-reaction complex' (RC), 'post-reaction complex' (PC), 'transition states' (TS), 'intermediates' (IM) and 'products' (P).

2.3 Kinetics Calculations. MultiWell 2014.1 software was employed to simulate the reaction kinetics (Barker et al., 2014; Barker, 2001). Rate constants for the multi-channel and multi-well chemical reactions involving tight transition states were calculated using Rice-Ramsberger-Kassel-Marcus (RRKM) theory (Barker, 2001), while those for barrierless reactions were obtained with long-range transition-state theory with a dispersion force potential or Inverse Laplace Transformation (ILT) model. Full computational settings are provided in our previous studies (Ma et al., 2018; Ma et al., 2021). For single-step processes, canonical transition state theory (TST) in the Thermo module of MultiWell-2014.1 program suite was applied to calculate the rate constants. Tunneling corrections for H-shift or H-abstraction reactions were included via a one-dimensional asymmetric Eckart potential (Eckart, 1930). Reaction rate constants for ·Cl + imines reactions were performed across the temperature range of 260 – 330 K. The parameters used in the long-range transition-state theory (LRTST) calculations and Lennard-Jones parameters for various species used in the MultiWell are shown in Table S1 and S2, respectively.

3 Results and Discussion

3.1 ·Cl-Initiated Reactions. ·Cl can either abstract H atoms from the $=CH_x-$ (x = 1~2) and =NH groups or add to the C=N bond of the target imines. The calculated energetic data are summarized in Table 1, with the corresponding zero-point energy (ZPE) corrected potential energy surfaces (PES) shown in Figure S2. Based on the reaction activation energies (E_a) in Table 1, it can be concluded that H-abstractions at the N-sites is the most energetically favorable pathway for ·Cl-initiated reactions of CH_2=NH, CH_3CH=NH, $(CH_3)_2C$=NH, and $HN=CHCH_2OH$, which is similar to amines + ·Cl systems (Ma et al., 2018; Xue et al., 2022; Xie et al., 2015; Xie et al., 2017). Notably, the E_a values for the formation of N-centered radicals from imines are significantly higher than those from amines. Interestingly, ·OH-initiated reactions of CH_2=NH can also result in the formation of N-centered radical, unlike ·OH-initiated reactions of amines, although the E_a value for the ·OH + CH_2=NH reaction being approximately 4 kcal mol^{-1} higher than that of ·Cl + CH_2=NH reaction (Bunkan et al., 2014). For $CH_3N=CH_2$, H-abstraction from the CH_2 site forming C-centered radical is the most favorable pathway, consistent with ·OH + $CH_3N=CH_2$ system (Bunkan et al., 2022).

It should be noted that, despite numerous attempts, the TSs for H-abstraction from the CH_2 site of $CH_3N=CH_2$ and for ·Cl addition to the N site of $(CH_3)_2C$=NH could not be located at the MP2/6-31+G(3df,2p) level. By analyzing the thermodynamic data, we found that ·Cl addition to the N-site is thermodynamically unfavorable for the ·Cl + $(CH_3)_2C$=NH reactions, suggesting that this pathway plays

a negligible role. For $(CH_3)_2C=NH$, the TS_{3-2} of ·Cl abstracting a H-atom from CH_2 site was located at the MP2/6-31+G(d,p) level. To evaluate the performance of the MP2/6-31+G(d,p) method for geometry optimization and CCSD(T)/6-311+G(2df,2p) for single point energy calculation in calculating the reaction energies (E_a and ΔE) of H-abstraction at the CH_2 site of $CH_3N=CH_2$, we randomly selected a pathway involved TS_{3-1} to calculate the E_a and ΔE values using the CCSD(T)/6-311+G(2df,2p)//MP2/6-31+G(d,p) and CCSD(T)/aug-cc-pVTZ//MP2/6-31+G(3df,2p) methods. The results show that the difference in E_a and ΔE values between the CCSD(T)/aug-cc-pVTZ//MP2/6-31+G(3df,2p) and CCSD(T)/6-311+G(2df,2p)//MP2/6-31+G(d,p) were within the quantum chemistry method (1.0 mol^{-1}) (Table S3). These indicate that the more efficient CCSD(T)/6-311+G(2df,2p)//MP2/6-31+G(d,p) method is reliable, and the E_a values of TS_{3-2} obtained with this method have negligible effects on the conclusions.

Table 1. Calculated reaction activation energies (E_a, in kcal mol^{-1}), thermodynamic energies (ΔE, kcal mol^{-1}), branch ratios (Γ) and reaction rate constants (k_{Cl}, in cm^3 $molecule^{-1}$ s^{-1}) for the reactions of ·Cl with **(a)** $CH_2=NH$, **(b)** $CH_3CH=NH$, **(c)** $CH_3N=CH_2$, **(d)** $(CH_3)_2C=NH$, and **(e)** $HN=CHCH_2OH$ at the CCSD(T)/aug-cc-pVTZ//MP2/6-31+G(3df,2p) level of theory.

	Species	TS	E_a	ΔE	Γ	$k_{Cl} \times 10^{-11}$
(a)	P_{1-1}	TS_{1-1}	2.35	0.08	0.26%	4.5
	P_{1-2}	TS_{1-2}	-0.60	-4.30	8.25%	
	P_{1-3}	TS_{1-3}	-4.39	-12.22	90.85%	
	P_{1-4}	TS_{1-4}	0.89	-13.13	0.64%	
	P_{1-5}	TS_{1-5}	5.14	8.97	0.00%	
(b)	P_{2-1}	TS_{2-1}	7.95	5.68	0.00%	27.2
	$P_{2-2/3}$	TS_{2-2}	2.26	-8.59	0.06%	
	$P_{2-2/3}$	TS_{2-3}	2.29	-8.59	0.05%	
	P_{2-4}	TS_{2-4}	-2.22	-5.15	11.96%	
	P_{2-5}	TS_{2-5}	-5.99	-10.55	87.58%	
	P_{2-6}	TS_{2-6}	-0.85	-11.12	0.35%	
	P_{2-7}	TS_{2-7}	6.57	8.46	0.00%	
(c)	P_{3-1}	TS_{3-1}	1.91	1.87	0.16%	7.32
	P_{3-2}	TS_{3-2}	-2.57[a]	-1.66[a]	59.37%	
	P_{3-3}	TS_{3-3}	-1.67	-2.01	32.98%	
	$P_{3-4/5}$	$TS_{3-4/5}$	1.39	-12.00	0.98%/0.98%	
	P_{3-6}	TS_{3-6}	-1.22	-15.02	5.53%	
	P_{3-7}	TS_{3-7}	4.26	8.19	0.00%	
(d)	P_{4-1}	TS_{4-1}	6.31	4.35	0.00%	44.8
	$P_{4-2/3}$	$TS_{4-2/3}$	0.89	-6.82	0.01%/0.01%	
	P_{4-4}	TS_{4-4}	4.19	2.94	0.00%	
	$P_{4-5/6}$	$TS_{4-5/6}$	1.21	-7.13	0.01%/0.01%	
	P_{4-7}	TS_{4-7}	-6.87	-10.35	99.96%	
	P_{4-8}	TS_{4-8}	-1.40	-10.53	0.00%	
	P_{4-9}	TS_{4-9}	——	12.43	——	
(e)	$P_{5-1/2}$	$TS_{5-1/2}$	-1.13	-20.52	6.08%/6.08%	12.6
	P_{5-3}	TS_{5-3}	-1.53	-2.98	39.46%	
	P_{5-4}	TS_{5-4}	-2.59	-6.96	48.33%	
	P_{5-5}	TS_{5-5}	15.09	9.69	0.00%	
	P_{5-6}	TS_{5-6}	1.16	-8.83	0.05%	
	P_{5-7}	TS_{5-7}	9.42	12.23	0.00%	

[a]Energies were calculated at the CCSD(T)/6-311+G(2df,2p)//MP2/6-31+G(d,p) level.

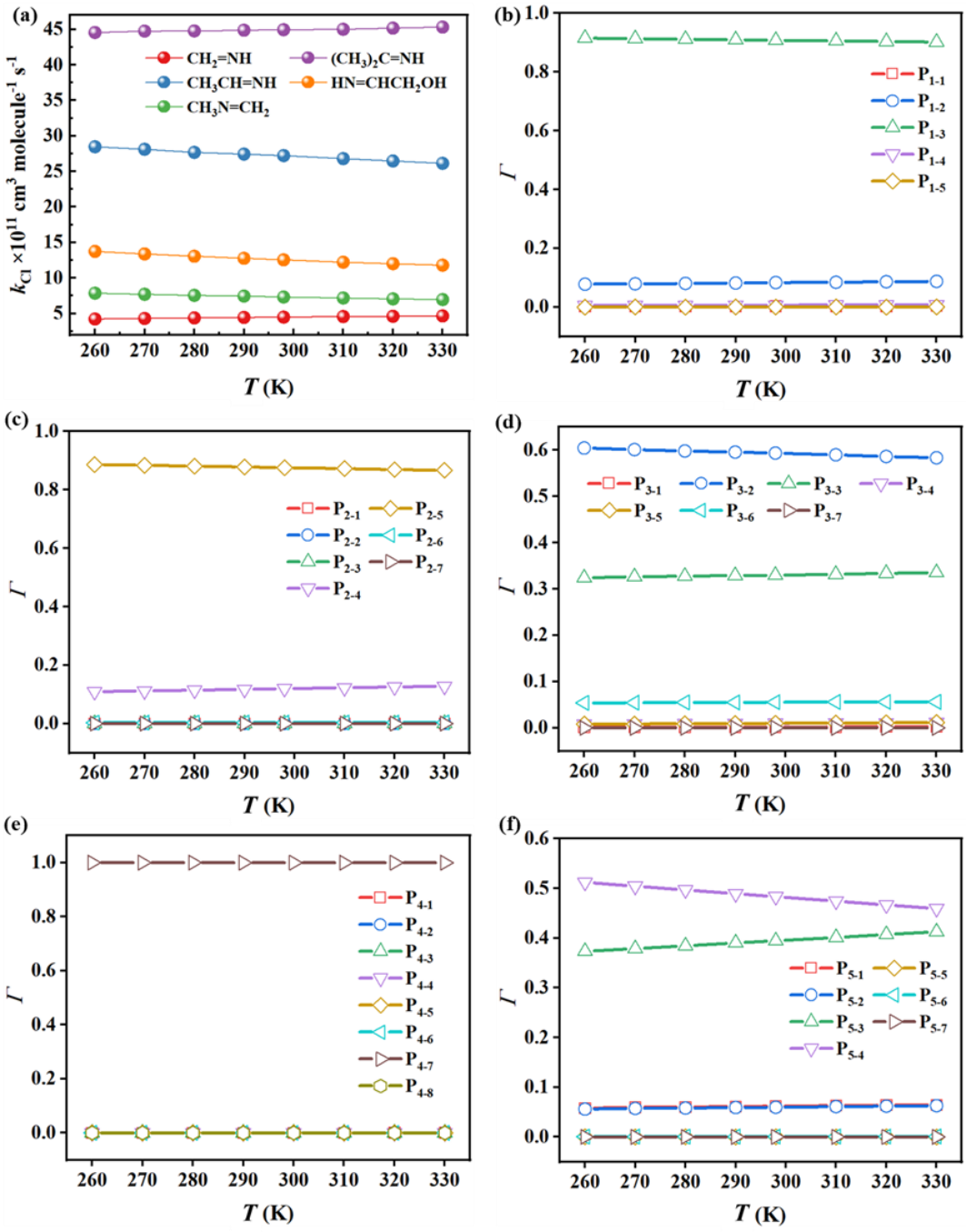

Figure 1. Reaction rate constants (k_{Cl}) for the reactions of five imines **(a),** and branching ratios (Γ) for products for the reactions of **(b)** CH_2=NH, **(c)** CH_3CH=NH, **(d)** CH_3N=CH_2, **(e)** $(CH_3)_2$C=NH, and **(f)** HN=$CHCH_2OH$ initiated by ·Cl in the temperature range of 260 – 300 K at 1 atm.

Since ·Cl abstracts a H-atom from sp^2-N site is more favorable than from other sites, it merits further discussion why the E_a values for generating N-centered radicals are substantially lower than those for C-centered radicals. By analyzing NBO charges for all TSs, we found that larger charge transfers occurred at the most favorable transition states TS_{1-3} (-0.428 *e*), TS_{2-5} (-0.447 *e*), TS_{3-2} (-0.318 *e*) and TS_{4-7} (-0.456 *e*) than other TSs (see Table S4). This indicates that charge transfer contributes critically to the stabilization of these TSs, thereby facilitating the formation of N-centered radicals in ·Cl-initiated reactions of NH-containing imines. A similar phenomenon was observed in the piperazine (PZ) + ·Cl

system (Ma et al., 2018). However, in the case of ·Cl + HN=CHCH$_2$OH system, the charge transfer at the TS$_{5\text{-}5}$ (-0.430 *e*) is slightly larger than that at the TS$_{5\text{-}4}$ (the most favorable one, -0.423 *e*) (see Table S4). The presence of intermolecular hydrogen bonds in TS$_{5\text{-}4}$ may account for its lower E_a value (see Figure S3).

Using the master equation approach, the overall rate constants (k_{Cl}) were determined to be 4.50 × 10^{-11}, 2.72 × 10^{-10}, 7.32 × 10^{-11}, 4.48 × 10^{-10} and 1.26 × 10^{-10} cm^3 molecule^{-1} s^{-1} for ·Cl + CH$_2$=NH, ·Cl + CH$_3$CH=NH, ·Cl + CH$_3$N=CH$_2$, ·Cl + (CH$_3$)$_2$C=NH, and ·Cl + HN=CHCH$_2$OH reactions at 298 K and 1 atm, respectively. The experimental k_{Cl} value available for the CH$_3$N=CH$_2$ + ·Cl reaction is (1.9 ± 0.15) × 10^{-11} cm^3 molecule^{-1} s^{-1} (Bunkan et al., 2022), which in good consistency with the corresponding computational result (7.32 × 10^{-11} cm^3 molecule^{-1} s^{-1}). This could further support the reliability of our computational approach. Over the temperature range of 260 – 330 K, CH$_2$=NH and (CH$_3$)$_2$C=NH show positive temperature dependence for k_{Cl}, whereas CH$_3$CH=NH, CH$_3$N=CH$_2$ and HN=CHCH$_2$OH exhibit a negative dependence (Figure 1a). By analyzing the substitutions effects on the k_{Cl} values, it can be found that -CH$_3$ and -(CH$_3$)$_2$ substitutions at the >**C**R1= position, as well as the -CH$_3$ substitution at the =**N**R2 position, increase the k_{Cl} values, while substitutions at the R3**C**CH= position have little effect on the k_{Cl} values.

The calculated Γ values for the N-centered radicals in the reactions of ·Cl + CH$_2$=NH, ·Cl + CH$_3$CH=NH, ·Cl + (CH$_3$)$_2$C=NH and ·Cl + HN=CHCH$_2$OH are 90.85%, 87.58%, 99.96% and 48.33% at 1 atm and 298 K, respectively. The Γ values of N-centered radicals show a slight decrease with increasing temperature, whereas those of other product species remain very small and negligible across the studied temperature range (Figure 1b, 1c, 1e and 1f). Therefore, N-centered radicals are the main products in these four reactions under atmospheric conditions, similar to ·Cl + amines systems (Ma et al., 2018; Xie et al., 2015). For the ·Cl + CH$_3$N=CH$_2$ reaction, the calculated Γ values for P$_{3\text{-}1}$, P$_{3\text{-}2}$, P$_{3\text{-}3}$, P$_{3\text{-}4/5}$, P$_{3\text{-}6}$, and P$_{3\text{-}7}$ are 0.16%, 59.36%, 32.98%, 0.98%, 5.53%, 0.00%, respectively, indicating a strong preference for the formation of C-centered radicals (Figure 1d). Since previous study have investigated the transformation of CH$_3$N=CH· (P$_{3\text{-}2}$) (Bunkan et al., 2022), we mainly considered the further transformation of the formed four N-centered radicals in the subsequent sections.

3.2 Subsequent Reactions of the formed N-centered radicals.

Consistent with previously studied N-centered radicals (Ma et al., 2018; Xie et al., 2015; Da Silva, 2013; Tang and Nielsen, 2012), the four N-centered radicals (CH$_2$=N·, CH$_3$CH=N·, (CH$_3$)$_2$C=N·, and ·N=CHCH$_2$OH) will subsequently undergo self-isomerization/dissociation or react with key atmospheric oxidants, such as O$_2$ and NO. From the calculated ZPE-corrected PES of self-isomerization/dissociation for these four N-centered radicals (Figure S4), it can be found that the E_a values are in the range of 27.85 – 79.58 kcal mol^{-1}, suggesting that both the self-isomerization and dissociation processes proceed very slowly. Therefore, in the atmosphere, these four N-centered radicals are more likely to react with O$_2$ and NO.

Regarding the reactions of the four N-centered radicals with O$_2$, two distinct routes were identified. The first pathway involves O$_2$ directly abstracting a H-atom from =CH$_x$– (x = 1~2) and –CH$_3$ sites, forming cyanide compounds, cyclic imines and HO$_2$·. The second pathway proceeds by O$_2$ addition to

the =N– site, with E_a values in the range of 5.60 – 14.18 kcal mol^{-1}, forming adducts with various conformations depending on the direction of O_2 attack. The calculated ZPE-corrected PES for the four N-centered radicals + O_2 reactions are shown in Figure 2. With the exception of $(CH_3)_2C=N\cdot$, the E_a values for the direct H-abstraction pathways in the $CH_2=N\cdot$ + O_2, $CH_3CH=N\cdot$ + O_2, and $\cdot N=CHCH_2OH$ + O_2 reactions are 12.25, 10.86 and 10.89 kcal mol^{-1}, respectively, significantly lower than those of addition pathways. Therefore, the H-abstraction pathway represents the primary pathway for these three reactions, producing cyanide compounds and $HO_2\cdot$. A similar direct H-abstraction mechanism has been observed in the reactions of N-centered radicals formed from amines with O_2 (Ma et al., 2018; Xue et al., 2022; Xie et al., 2015; Xie et al., 2017). For $(CH_3)_2C=N\cdot$, the E_a value of O_2 addition forming $IM_{12\text{-}1}$ is lower than that for the direct H-abstraction pathways. Therefore, the formation of adduct $IM_{12\text{-}1}$ is most favorable in the initial attack of O_2. However, the $IM_{12\text{-}1}$ is unstable and will readily reverts to $(CH_3)_2C=N\cdot$ and O_2, making it difficult to react with O_2.

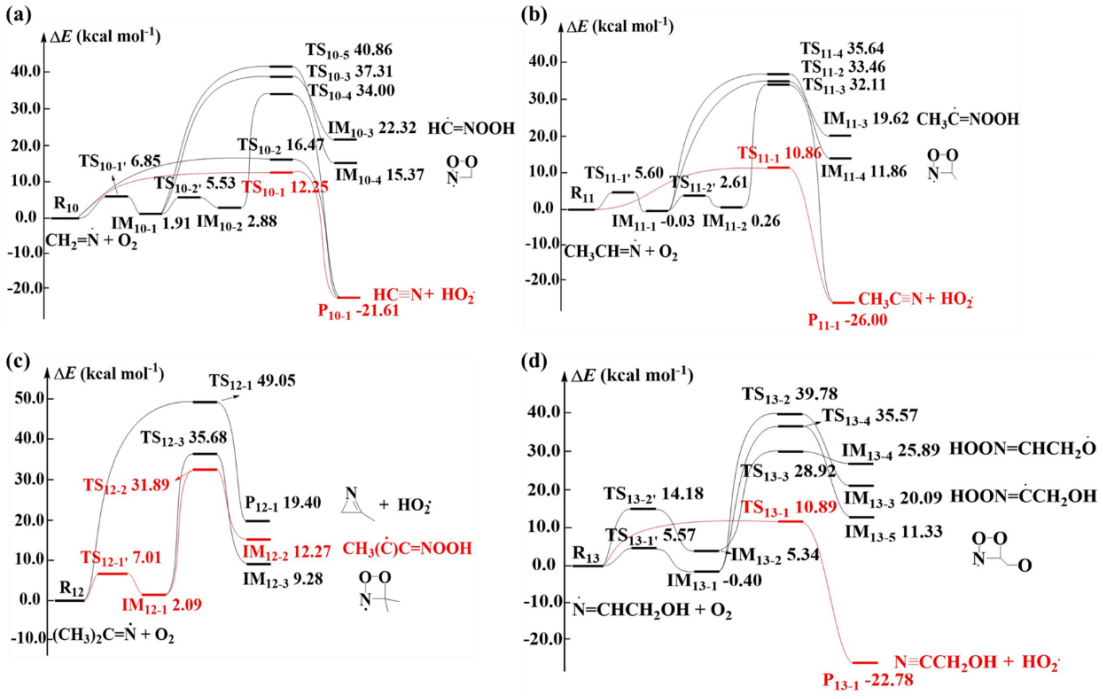

Figure 2. Schematic ZPE-corrected PES for the reactions of O_2 with **(a)** $CH_2=N\cdot$, **(b)** $CH_3CH=N\cdot$, **(c)** $(CH_3)_2C=N\cdot$, and **(d)** $\cdot N=CHCH_2OH$ at the CCSD(T)/6-311+G(2df,2p)//M06-2X/6-31+G(d,p) level of theory.

Our previous studies revealed that E_a values of O_2 directly abstracting H-atoms from N-centered radicals is highly sensitive to the employed theorical methods, which ultimately affects the reaction rate constant (k_{O2}) with O_2 (Liu et al., 2019; Xie et al., 2017). Since k_{O2} is a key parameter in determining nitrosamines yields in subsequent reactions (Liu et al., 2019; Wang, 2015), we further evaluated the impact of different computational approaches on the E_a values for direct H-abstraction pathways. The E_a values obtained at CCSD(T)/aug-cc-pVTZ//MP2/6-31+G(3df,2p), CCSD(T)/aug-cc-pVTZ//MP2/aug-cc-pVTZ and CCSD(T)/6-311+G(2df,2p)//M06-2X/6-31+G(d,p) are summarized in Table S5. When the geometry optimization method was changed from M06-2X/6-31+G(d,p) to MP2/6-31+G(3df,2p) or MP2/aug-cc-pVTZ, and the single point energy calculation was changed from CCSD(T)/6-311+G(2df,2p)

to CCSD(T)/aug-cc-pVTZ, the deviations in E_a values reach up to 6.2 kcal mol^{-1} [between CCSD(T)/aug-cc-pVTZ//MP2/6-31+G(3df,2p) and CCSD(T)/6-311+G(2df,2p)//M06-2X/6-31+G(d,p)] and 6.4 kcal mol^{-1} [between CCSD(T)/aug-cc-pVTZ//MP2/aug-cc-pVTZ and CCSD(T)/6-311+G(2df,2p)//M06-2X/6-31+G(d,p)]. By contrast, changing the optimization method from MP2/6-31+G(3df,2p) to MP2/aug-cc-pVTZ lead to only 0.3 kcal mol^{-1} deviation of E_a values between CCSD(T)/aug-cc-pVTZ//MP2/6-31+G(3df,2p) and CCSD(T)/aug-cc-pVTZ//MP2/aug-cc-pVTZ. These results indicate that the combination of the computationally cheaper M06-2X and CCSD(T) does not provide accurate results for these systems. Therefore, the E_a values calculated at the CCSD(T)/aug-cc-pVTZ//MP2/6-31+G(3df,2p) level were adopted for subsequent kinetics calculations. Notably, H-abstraction in the CH_2=N· + O_2, CH_3CH=N· + O_2, and ·N=$CHCH_2OH$ + O_2 systems remain the most favorable reaction pathways even at higher CCSD(T)/aug-cc-pVTZ//MP2/6-31+G(3df,2p) methods.

Since E_a values of the direct H-abstraction pathways are notably lower than those of the addition pathways for CH_2=N·, CH_3CH=N· and ·N=$CHCH_2OH$, the overall k_{O2} are approximated to be the rate constants of the direct H-abstraction pathways. The TST was applied to examine the kinetics of the direct H-abstraction pathways. The calculated k_{O2} of the direct H-abstraction pathway for CH_2=N· + O_2, CH_3CH=N· + O_2 and ·N=$CHCH_2OH$ + O_2 reactions based on the energies calculated at the CCSD(T)/aug-cc-pVTZ//MP2/6-31+G(3df,2p) level are 8.94×10^{-18}, 1.15×10^{-17} and 1.38×10^{-17} cm^3 molecule^{-1} s^{-1} at 298 K, respectively. The k_{O2} values of these three N-centered radicals formed from imines oxidation are similar to or higher than those of chain- and cyclic-like N-centered radicals from amines oxidation (Ma et al., 2018; Liu et al., 2019; Xie et al., 2015). Therefore, the k_{O2} values for N-centered radicals with O_2 varies greatly with their specific molecular structures. Previous studies have shown that the reactions of amines-derived N-centered radicals with O_2 can compete with their reactions with NO under typical tropospheric NO concentrations (Ma et al., 2018). Therefore, we further investigated the reactions of these four N-centered radicals (CH_2=N·, CH_3CH=N·, $(CH_3)_2C$=N· and ·N=$CHCH_2OH$) with NO.

The calculated ZPE-corrected PES for the reactions of these four N-centered radicals with NO are presented in Figure 3. As shown in Figure 3, two types of reaction pathways are observed during the initial interaction of NO with the N-centered radicals. The first is the direct H-abstraction pathway, where NO abstracts a H-atom from the =CH_x– (x = 1~2) sites adjacent to the =N– and –CH_3 groups. These H-abstraction pathways need to overcome at least 13.35 kcal mol^{-1} E_a values to form cyanide compounds and HNO. The second is the NO addition pathway, where NO barrierlessly addition to the =N– site of the four N-centered radicals, forming nitrosamines adducts with different conformations depending on the approach direction of NO. Interconversion between these adducts, such as IM_{14-1} and IM_{14-2}, IM_{15-1} and IM_{15-2}, IM_{17-1} and IM_{17-2} proceeds with very low energy barriers of 0.53, 1.42 and 1.68 kcal mol^{-1}, respectively.

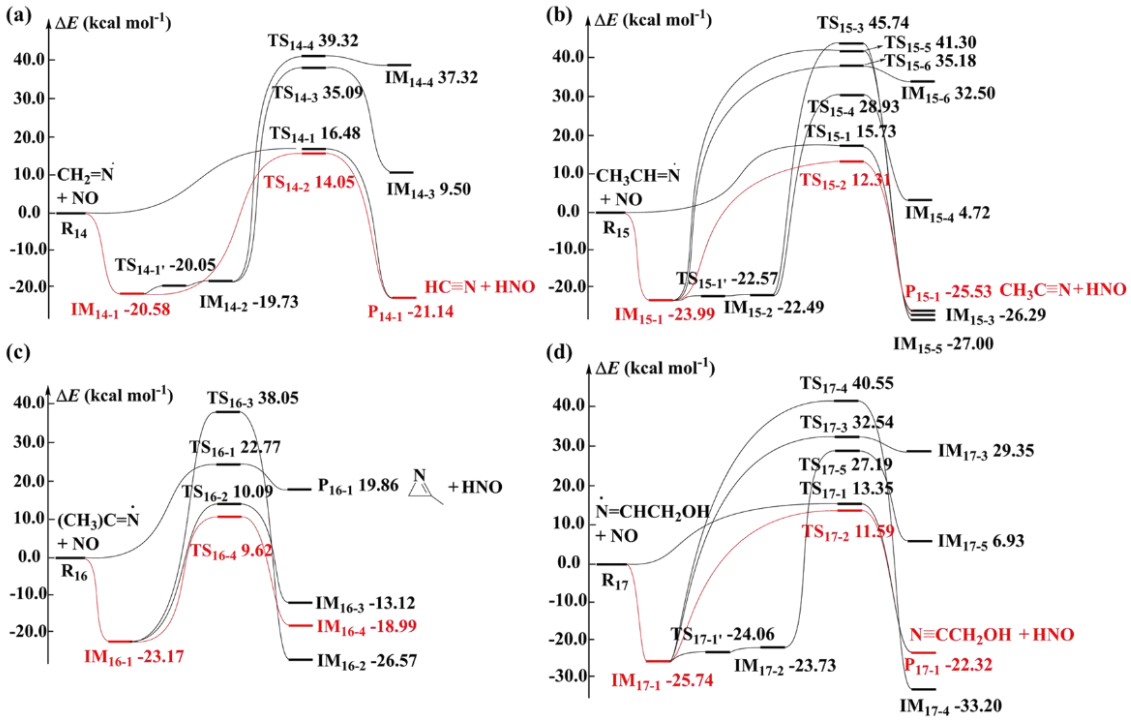

Figure 3. Schematic ZPE-corrected PES for the reactions of NO with **(a)** CH_2=N·, **(b)** CH_3CH=N·, **(c)** $(CH_3)_2C$=N·, and **(d)** ·N=$CHCH_2OH$ at the CCSD(T)/6-311+G(2df,2p)//M06-2X/6-31+G(d,p) level of theory.

The formed four adducts (nitrosamines) can further undergo isomerization or dissociation reactions. For $IM_{14\text{-}1}$/$IM_{14\text{-}2}$, $IM_{15\text{-}1}$/$IM_{15\text{-}2}$, $IM_{16\text{-}1}$, $IM_{17\text{-}1}$/$IM_{17\text{-}2}$, three, five, three and four H-shift pathways are identified, respectively. It is observed that H-shifts from the =CH_x– (x = 1~2) sites adjacent to the =N– and –CH_3 groups to the O-atom of the –NNO group are the most favorable. However, the formed four adducts need to overcome high energy barriers to isomerize or dissociate into fragmentation products. This mechanism is analogous to amines-derived N-centered radicals with NO. In addition, the main reaction pathway remains even at high computational methods (see Table S6 and S7).

To maintain consistency with the N-centered + O_2 reactions, the reaction energies calculated at the CCSD(T)/aug-cc-pVTZ//MP2/6-31+G(3df,2p) level are used to calculate the reaction rate constant (k_{NO}) for the reactions of four N-centered radicals with NO. The calculated reaction rate constants for NO addition pathways for the reactions of CH_2=N· + NO, CH_3CH=N· + NO, $(CH_3)_2C$=N· + NO and ·N=$CHCH_2OH$ + NO are 2.20×10^{-16}, 1.42×10^{-12}, 1.09×10^{-10} and 4.30×10^{-11} cm^3 $molecule^{-1}$ s^{-1} at 298 K, respectively. These are much higher than those for the corresponding direct H-abstraction pathways (1.85×10^{-21}, 2.87×10^{-21}, 5.57×10^{-27} and 1.04×10^{-19} cm^3 $molecule^{-1}$ s^{-1}). Therefore, the k_{NO} can be assumed to be equal to the reaction rate constant for the addition pathways. The calculated Γ values for the nitrosamine ($IM_{14\text{-}1}$, $IM_{15\text{-}1}$, $IM_{16\text{-}1}$ and $IM_{17\text{-}1}$) for the reactions of CH_2=N· + NO, CH_3CH=N· + NO, $(CH_3)_2C$=N· + NO and ·N=$CHCH_2OH$ + NO are 0.08%, 6.22%, 52.56% and 35.32% at 1 atm and 298 K, respectively. Consequently, except for CH_2=N· and CH_3CH=N·, the reactions of $(CH_3)_2C$=N· and ·N=$CHCH_2OH$ with NO can lead to carcinogenic nitrosamines with high yields. It is noteworthy that the Γ values for nitrosamine formation in these two reactions are significantly lower than

those of PZ-N (99.97%) (Ma et al., 2018), Monoethanolamine (MEA)-N (86%) (Xie et al., 2015) and $CH_3NH\cdot$ (~60%) (Da Silva, 2013) with NO.

Since $(CH_3)_2C{=}N\cdot$ exclusively reaction with NO, we only assessed the competition of O_2 and NO for other three N-centered radicals using the calculated k_{O2} and k_{NO} values. The required concentrations of NO ([NO]) to equalize the pseudo-first-order rate constants for N-centered radicals with O_2 are 8.1×10^6, 1.7×10^3 and 64 ppb, respectively. For $CH_2{=}N\cdot$ and $CH_3CH{=}N\cdot$, the required [NO] are very high, far exceeding the typical [NO] encountered in the atmosphere (Ren, 2003). Therefore. $CH_2{=}N\cdot$ and $CH_3CH{=}N\cdot$ are expected to primarily react with O_2 to form HC≡N and $CH_3C{\equiv}N$, respectively, consistent with previous studies of CH_2=NH (Bunkan et al., 2014). In contrast, for $\cdot N{=}CHCH_2OH$, the required [NO] are achievable under polluted atmospheric conditions. Therefore, both $(CH_3)_2C{=}N\cdot$ and $\cdot N{=}CHCH_2OH$ can react with NO to form nitrosamines. To the best of knowledge, this study represents the first report demonstrating that N-centered radicals formed from ·OH-initiated reactions of imines can lead to carcinogenic nitrosamine formation. However, the yields of nitrosamine formation are highly dependent on the specific structures of N-centered radicals.

4 Conclusions

Similar to previous studies on amines + ·Cl reaction systems, the reaction of imines containing =NH (CH_2=NH, CH_3CH=NH, $(CH_3)_2C$=NH, and $HN{=}CHCH_2OH$) with ·Cl predominantly yield N-centered radicals. The calculated k_{Cl} values for the reactions of CH_2=NH, CH_3CH=NH, $CH_3N{=}CH_2$, $(CH_3)_2C$=NH, and $HN{=}CHCH_2OH$ are 4.50×10^{-11}, 2.72×10^{-10}, 7.32×10^{-11}, 4.48×10^{-10} and 1.26×10^{-10} cm^3 $molecule^{-1}$ s^{-1} at 298 K and 1 atm, respectively. Among the five imines studied, only the reaction kinetics of CH_2=NH and $CH_3N{=}CH_2$ with ·OH are available (CH_2=NH: 3.00×10^{-12} cm^3 $molecule^{-1}$ s^{-1}, $CH_3N{=}CH_2$: 3.70×10^{-12} cm^3 $molecule^{-1}$ s^{-1}). With these data, we can estimate the contribution of ·Cl to the degradation of CH_2=NH and $CH_3N{=}CH_2$ based on the ·Cl concentration ([·Cl]). In the marine boundary layer, the [·Cl] is typically 1 – 10% of the [·OH]. The contribution of ·Cl relative to ·OH (k_{Cl}[·Cl]/k_{OH}[·OH]) to the transformation of CH_2=NH and $CH_3N{=}CH_2$ are estimated to be 15% – 150% and 20% – 200%, respectively. Furthermore, the contribution of ·Cl relative to ·OH to the formation of $CH_2{=}N\cdot$ is estimated at 34% – 340% (estimated by k_{Cl}[·Cl] × $\Gamma_{N,Cl}$ /k_{OH}[·OH] × $\Gamma_{N,OH}$, where $\Gamma_{N,Cl}$ and $\Gamma_{N,OH}$ represent the yields of N-centered radicals from the reactions initiated by ·Cl and ·OH, respectively) This clearly demonstrates the significant role of ·Cl in the transformation of CH_2=NH and $CH_3N{=}CH_2$. Although complete data on the reactions of other imines (CH_3CH=NH, $(CH_3)_2C$=NH, and $HN{=}CHCH_2OH$) with ·OH are lacking, it is reasonable to believe that ·Cl also plays a crucial role in their transformation based on their high k_{Cl} values.

Unlike N-centered radicals generated from amines oxidation, this study reveals that both k_{O2} and k_{NO} values for N-centered radicals generated from imines oxidation are strongly dependent on their specific structures, ultimately affecting nitrosamine formation. This study provides the first evidence that N-centered radicals formed from imines oxidation can yield nitrosamines under polluted atmospheric conditions. Therefore, to comprehensively evaluate the formation of nitrosamines from imines, further investigations into the reactions of imine-derived N-centered radicals with O_2 and NO are warranted.

Data availability. All data were available in the main text or supplementary materials. The other relevant data are available upon request from the corresponding authors.

Author contribution. HBX and MFF designed research; XQ, MFF and HBX performed research; XQ, MFF, LC, ZQJ and HBX analyzed data; XQ and MFF wrote the paper; XQ, MFF, CJW and HBX reviewed and revised the paper.

Competing interests. The authors declare that they have no conflict of interest.

Acknowledgements. The study was supported by the National Natural Science Foundation of China (22206020, 22236004, 22176022), the National Key Research and Development Program of China (2022YFC3701000), and the Sugon Supercomputing Center.

References

Abudumutailifu, M., Shang, X., Wang, L., Zhang, M., Kang, H., Chen, Y., Li, L., Ju, R., Li, B., Ouyang, H., Tang, X., Li, C., Wang, L., Wang, X., George, C., Rudich, Y., Zhang, R., and Chen, J.: Unveiling the Molecular Characteristics, Origins, and Formation Mechanism of Reduced Nitrogen Organic Compounds in the Urban Atmosphere of Shanghai Using a Versatile Aerosol Concentration Enrichment System, Environ. Sci. Technol., 58, 7099-7112, 10.1021/acs.est.3c04071, 2024.

Akbar Ali, M., M., B., and Lin, K. C.: Catalytic effect of a single water molecule on the OH + CH_2NH reaction, Phys. Chem. Chem. Phys., 20, 4297-4307, 10.1039/C7CP07091H, 2018.

Ali, M. A.: Computational studies on the gas phase reaction of methylenimine (CH_2NH) with water molecules, Sci. Rep., 10, 10995, 10.1038/s41598-020-67515-3, 2020.

Ali, M. A., Sonk, J. A., and Barker, J. R.: Predicted Chemical Activation Rate Constants for HO_2 + CH_2 NH: The Dominant Role of a Hydrogen-Bonded Pre-reactive Complex, J. Phys. Chem. A, 120, 7060-7070, 10.1021/acs.jpca.6b06531, 2016.

Almeida, T. G., and Kurtén, T.: Atmospheric Oxidation of Imine Derivative of Piperazine Initiated by OH Radical, ACS Earth Space Chem., 6, 2453-2464, 10.1021/acsearthspacechem.2c00170, 2022.

Barker, J. R.: Multiple-Well, multiple-path unimolecular reaction systems. I. MultiWell computer program suite, Int. J. Chem. Kinet., 33, 232-245, 10.1002/kin.1017, 2001.

Barker, J. R., Ortiz, N. F., Preses, J. M., Lohr, L. L., Maranzana, A., Stimac, P. J., Nguyen, T. L., and Kumar, T. J. D.: MultiWell-2014, in, edited, 1, New York, 232-245, 2014.

Bunkan, A. J. C., Reijrink, N. G., Mikoviny, T., Müller, M., Nielsen, C. J., Zhu, L., and Wisthaler, A.: Atmospheric Chemistry of *N* -Methylmethanimine ($CH_3N{=}CH_2$): A Theoretical and Experimental Study, J. Phys. Chem. A, 126, 3247-3264, 10.1021/acs.jpca.2c01925, 2022.

Bunkan, A. J. C., Tang, Y., Sellevåg, S. R., and Nielsen, C. J.: Atmospheric Gas Phase Chemistry of $CH_2{=}NH$ and HNC. A First-Principles Approach, The Journal of Physical Chemistry A, 118, 5279-5288, 10.1021/jp5049088, 2014.

Cao, Y., Liu, J., Ma, Q., Zhang, C., Zhang, P., Chen, T., Wang, Y., Chu, B., Zhang, X., Francisco, J. S., and He, H.: Photoactivation of Chlorine and Its Catalytic Role in the Formation of Sulfate Aerosols, J. Am. Chem. Soc., 146, 1467-1475, 10.1021/jacs.3c10840, 2024.

Carey, F. A., and Sundberg, R. J.: Advanced Organic Chemistry FIFTH, in, edited, Springer Science & Business Media, 2007.

Chen, G., Fan, X., Lin, Z., Ji, X., Chen, Z., Xu, L., and Chen, J.: Driving factors and photochemical

impacts of Cl_2 in coastal atmosphere of Southeast China, npj Clim. Atmos. Sci., 8, 135, 10.1038/s41612-025-01022-y, 2025.

Chen, X., Jiang, Y., Zong, Z., Wang, Y., Sun, W., Wang, Y., Xia, M., Guan, L., Liu, P., Zhang, C., Chen, J., Mu, Y., and Wang, T.: Atmospheric Reactive Halogens Reshaped by the Clean Energy Policy and Agricultural Activity in a Rural Area of the North China Plain, Environ. Sci. Technol., 59, 12775-12785, 10.1021/acs.est.4c13986, 2025.

Cooke, M. E., Dam, M., Wingen, L. M., Perraud, V., Thomas, A. E., Rojas, B., Nagalingam, S., Ezell, M. J., La Salle, S., Bauer, P. S., Finlayson-Pitts, B. J., and Smith, J. N.: Emissions of Nitrous Acid, Nitryl Chloride, and Dinitrogen Pentoxide Associated with Automotive Braking, Environ. Sci. Technol., 59, 9167-9177, 10.1021/acs.est.4c13202, 2025.

Da Silva, G.: Formation of Nitrosamines and Alkyldiazohydroxides in the Gas Phase: The CH3NH + NO Reaction Revisited, Environ. Sci. Technol., 47, 7766-7772, 10.1021/es401591n, 2013.

Ding, Z., Tian, S., Dang, J., and Zhang, Q.: New mechanistic understanding for atmospheric oxidation of isoprene initiated by atomic chlorine, Sci. Total Environ., 801, 149768, 10.1016/j.scitotenv.2021.149768, 2021.

Ditto, J. C., Joo, T., Slade, J. H., Shepson, P. B., Ng, N. L., and Gentner, D. R.: Nontargeted Tandem Mass Spectrometry Analysis Reveals Diversity and Variability in Aerosol Functional Groups across Multiple Sites, Seasons, and Times of Day, Environ. Sci. Technol. Lett., 7, 60-69, 10.1021/acs.estlett.9b00702, 2020.

Ditto, J. C., Machesky, J., and Gentner, D. R.: Analysis of reduced and oxidized nitrogen-containing organic compounds at a coastal site in summer and winter, Atmos. Chem. Phys., 22, 3045-3065, 10.5194/acp-22-3045-2022, 2022.

Eckart, C.: The Penetration of a Potential Barrier by Electrons, Phys. Rev., 35, 1303-1309, 10.1103/PhysRev.35.1303, 1930.

Edwards, P. M., and Young, C. J.: Primary Radical Effectiveness: Do the Different Chemical Reactivities of Hydroxyl and Chlorine Radicals Matter for Tropospheric Oxidation? ACS ES&T Air, 1, 780-788, 10.1021/acsestair.3c00108, 2024.

Elm, J., Jen, C. N., Kurtén, T., and Vehkamäki, H.: Strong Hydrogen Bonded Molecular Interactions between Atmospheric Diamines and Sulfuric Acid, J. Phys. Chem. A, 120, 3693-3700, 10.1021/acs.jpca.6b03192, 2016.

Faxon, C. B., and Allen, D. T.: Chlorine chemistry in urban atmospheres: a review, Environ. Chem., 10, 221, 10.1071/EN13026, 2013.

Frisch, M. J., Trucks, G. W., Schlegel, H. B., Scuseria, G. E., Robb, M. A., Cheeseman, J. R., Scalmani, G., Barone, V., Petersson, G. A., Nakatsuji, H., Li, X., Caricato, M., Marenich, A. V., Bloino, J., Janesko, B. G., Gomperts, R., Mennucci, B., Hratchian, H. P., Ortiz, J. V., Izmaylov, A. F., Sonnenberg, J. L., Williams-Young, D., Ding, F., Lipparini, F., Egidi, F., Goings, J., Peng, B., Petrone, A., Henderson, T., Ranasinghe, D., Zakrzewski, V. G., Gao, J., Rega, N., Zheng, G., Liang, W., Hada, M., Ehara, M., Toyota, K., Fukuda, R., Hasegawa, J., Ishida, M., Nakajima, T., Honda, Y., Kitao, O., Nakai, H., Vreven, T., Throssell, K., Jr. Montgomery, J. A., Peralta, J. E., Ogliaro, F., Bearpark, M. J., Heyd, J. J., Brothers, E. N., Kudin, K. N., Staroverov, V. N., Keith, T. A., Kobayashi, R., Normand, J., Raghavachari, K., Rendell, A. P., Burant, J. C., Iyengar, S. S., Tomasi, J., Cossi, M., Millam, J. M., Klene, M., Adamo, C., Cammi, R., Ochterski, J. W., Martin, R. L., Morokuma, K., Farkas, O.,

Foresman, J. B., and Fox, D. J. G. I.: Gaussian 09, Revision A.02, Gaussian, Inc., Walling ford, CT, https://gaussian.com/g09citation/ (last access: 12 Dec 2025), 2009.

Fu, X., Wang, T., Wang, S., Zhang, L., Cai, S., Xing, J., and Hao, J.: Anthropogenic Emissions of Hydrogen Chloride and Fine Particulate Chloride in China, Environ. Sci. Technol., 52, 1644-1654, 10.1021/acs.est.7b05030, 2018.

Fu, Z., Guo, S., Xie, H., Zhou, P., Boy, M., Yao, M., and Hu, M.: A Near-Explicit Reaction Mechanism of Chlorine-Initiated Limonene: Implications for Health Risks Associated with the Concurrent Use of Cleaning Agents and Disinfectants, Environ. Sci. Technol., 58, 19762-19773, 10.1021/acs.est.4c04388, 2024.

Fukui, K.: The path of chemical reactions - the IRC approach, Acc. Chem. Res., 14, 363-368, 10.1021/ar00072a001, 1981.

Ge, X., Wexler, A. S., and Clegg, S. L.: Atmospheric amines – Part I. A review, Atmos. Environ., 45, 524-546, 10.1016/j.atmosenv.2010.10.012, 2011.

Gunthe, S. S., Liu, P., Panda, U., Raj, S. S., Sharma, A., Darbyshire, E., Reyes-Villegas, E., Allan, J., Chen, Y., Wang, X., Song, S., Pöhlker, M. L., Shi, L., Wang, Y., Kommula, S. M., Liu, T., Ravikrishna, R., McFiggans, G., Mickley, L. J., Martin, S. T., Pöschl, U., Andreae, M. O., and Coe, H.: Enhanced aerosol particle growth sustained by high continental chlorine emission in India, Nat. Geosci., 14, 77-84, 10.1038/s41561-020-00677-x, 2021.

Guo, X., Ma, F., Liu, C., Niu, J., He, N., Chen, J., and Xie, H.: Atmospheric oxidation mechanism and kinetics of isoprene initiated by chlorine radicals: A computational study, Sci. Total Environ., 712, 136330, 10.1016/j.scitotenv.2019.136330, 2020.

Li, C., Yao, L., Wang, Y., Fang, M., Chen, X., Wang, L., Li, Y., Yang, G., and Wang, L.: Formation of chlorinated organic compounds from Cl atom-initiated reactions of aromatics and their detection in suburban Shanghai, Atmos. Chem. Phys., 25, 11247-11260, 10.5194/acp-25-11247-2025, 2025.

Li, L., Yin, S., Huang, L., Yi, X., Wang, Y., Zhang, K., Ooi, C. G., and Allen, D. T.: An emission inventory for Cl_2 and HOCl in Shanghai, 2017, Atmos. Environ., 223, 117220, 10.1016/j.atmosenv.2019.117220, 2020.

Li, S., Liu, Y., Zhu, Y., Jin, Y., Hong, Y., Shen, A., Xu, Y., Wang, H., Wang, H., Lu, X., Fan, S., and Fan, Q.: ACEIC: a comprehensive anthropogenic chlorine emission inventory for China, Atmos. Chem. Phys., 24, 11521-11544, 10.5194/acp-24-11521-2024, 2024.

Liu, C., Ma, F., Elm, J., Fu, Z., Tang, W., Chen, J., and Xie, H.: Mechanism and predictive model development of reaction rate constants for N-center radicals with O_2, Chemosphere, 237, 124411, 10.1016/j.chemosphere.2019.124411, 2019.

Liu, L., Yu, F., Du, L., Yang, Z., Francisco, J. S., and Zhang, X.: Rapid sulfuric acid–dimethylamine nucleation enhanced by nitric acid in polluted regions, PNAS, 118, e2108384118, 10.1073/pnas.2108384118, 2021.

Liu, X., Liu, L., Zhang, B., Liu, P., Huang, R., Hildebrandt Ruiz, L., Miao, R., Chen, Q., and Wang, X.: Modeling the Global Impact of Chlorine Chemistry on Secondary Organic Aerosols, Environ. Sci. Technol., 58, 23064-23074, 10.1021/acs.est.4c05037, 2024.

Lu, R., Zhou, P., Ma, F., Zhao, Q., Peng, X., Chen, J., and Xie, H.: Multi-generation oxidation mechanism of M-xylene: Unexpected implications for secondary organic aerosol formation, Atmos. Environ., 327, 120511, 10.1016/j.atmosenv.2024.120511, 2024.

Molclus program, Version 1.9.3.: http://www.keinsci.com/research/molclus.html, (last accessed: 2025-12-12), 2025.

Ma, F., Ding, Z., Elm, J., Xie, H., Yu, Q., Liu, C., Li, C., Fu, Z., Zhang, L., and Chen, J.: Atmospheric Oxidation of Piperazine Initiated by ·Cl: Unexpected High Nitrosamine Yield, Environ. Sci. Technol., 52, 9801-9809, 10.1021/acs.est.8b02510, 2018.

Ma, F., Guo, X., Xia, D., Xie, H., Wang, Y., Elm, J., Chen, J., and Niu, J.: Atmospheric Chemistry of Allylic Radicals from Isoprene: A Successive Cyclization-Driven Autoxidation Mechanism, Environ. Sci. Technol., 55, 4399-4409, 10.1021/acs.est.0c07925, 2021.

Ma, F., Xie, H., Elm, J., Shen, J., Chen, J., and Vehkamäki, H.: Piperazine Enhancing Sulfuric Acid-Based New Particle Formation: Implications for the Atmospheric Fate of Piperazine, Environ. Sci. Technol., 53, 8785-8795, 10.1021/acs.est.9b02117, 2019.

Ma, F., Xie, H., Zhang, R., Su, L., Jiang, Q., Tang, W., Chen, J., Engsvang, M., Elm, J., and He, X.: Enhancement of Atmospheric Nucleation Precursors on Iodic Acid-Induced Nucleation: Predictive Model and Mechanism, Environ. Sci. Technol., 57, 6944-6954, 10.1021/acs.est.3c01034, 2023.

Ma, W., Feng, Z., Chen, X., Xia, M., Liu, Y., Zhang, Y., Liu, Y., Wang, Y., Zheng, F., Hua, C., Li, J., Zhao, Z., Yang, H., Kulmala, M., Worsnop, D. R., He, H., and Liu, Y.: Overlooked Significance of Reactive Chlorines in the Reacted Loss of VOCs and the Formation of O_3 and SOA, Environ. Sci. Technol., 59, 6155-6166, 10.1021/acs.est.4c10618, 2025.

Ning, A., Liu, L., Zhang, S., Yu, F., Du, L., Ge, M., and Zhang, X.: The critical role of dimethylamine in the rapid formation of iodic acid particles in marine areas, npj Clim. Atmos. Sci., 5, 1-9, 10.1038/s41612-022-00316-9, 2022.

Onel, L., Blitz, M., Dryden, M., Thonger, L., and Seakins, P.: Branching Ratios in Reactions of OH Radicals with Methylamine, Dimethylamine, and Ethylamine, Environ. Sci. Technol., 48, 9935-9942, 10.1021/es502398r, 2014.

Pople, J. A., Head-Gordon, M., Fox, D. J., Raghavachari, K., and Curtiss, L. A.: Gaussian-1 theory: A general procedure for prediction of molecular energies, J. Chem. Phys., 90, 5622-5629, 10.1063/1.456415, 1989.

Qiu, C., and Zhang, R.: Multiphase chemistry of atmospheric amines, Phys. Chem. Chem. Phys., 15, 5738-5752, 10.1039/c3cp43446j, 2013.

Reed, A. E., Weinstock, R. B., and Weinhold, F.: Natural population analysis, J. Chem. Phys., 83, 735-746, 10.1063/1.449486, 1985.

Ren, X.: HOx concentrations and OH reactivity observations in New York City during PMTACS-NY2001, Atmos. Environ., 37, 3627-3637, 10.1016/S1352-2310(03)00460-6, 2003.

Shen, X., Chen, J., Li, G., and An, T.: A new advance in the pollution profile, transformation process, and contribution to aerosol formation and aging of atmospheric amines, Environ Sci Atmos, 3, 444-473, 10.1039/D2EA00167E, 2023.

Sun, W., Hu, X., Fu, Y., Zhang, G., Zhu, Y., Wang, X., Yan, C., Xue, L., Meng, H., Jiang, B., Liao, Y., Wang, X., Peng, P., and Bi, X.: Different formation pathways of nitrogen-containing organic compounds in aerosols and fog water in northern China, Atmos. Chem. Phys., 24, 6987-6999, 10.5194/acp-24-6987-2024, 2024.

Tang, Y., and Nielsen, C. J.: A systematic theoretical study of imines formation from the atmospheric reactions of RnNH2−n with O_2 and NO_2 (R = CH_3 and CH_3CH_2; n = 1 and 2), Atmos. Environ., 55,

185-189, https://doi.org/10.1016/j.atmosenv.2012.02.094, 2012.

Thornton, J. A., Kercher, J. P., Riedel, T. P., Wagner, N. L., Cozic, J., Holloway, J. S., Dubé, W. P., Wolfe, G. M., Quinn, P. K., Middlebrook, A. M., Alexander, B., and Brown, S. S.: A large atomic chlorine source inferred from mid-continental reactive nitrogen chemistry, Nature, 464, 271-274, 10.1038/nature08905, 2010.

Vereecken, L., and Francisco, J. S.: Theoretical studies of atmospheric reaction mechanisms in the tropospherew, Chem. Soc. Rev., 41, 6259-6293, doi.org/10.1039/C2CS35070J, 2012.

Wang, C., Liggio, J., Wentzell, J. J. B., Jorga, S., Folkerson, A., and Abbatt, J. P. D.: Chloramines as an important photochemical source of chlorine atoms in the urban atmosphere, PNAS, 120, e2074078176, 10.1073/pnas.2220889120, 2023.

Wang, D. S., Masoud, C. G., Modi, M., and Hildebrandt Ruiz, L.: Isoprene–Chlorine Oxidation in the Presence of NO*x* and Implications for Urban Atmospheric Chemistry, Environ. Sci. Technol., 56, 9251-9264, 10.1021/acs.est.1c07048, 2022.

Wang, L.: The Atmospheric Oxidation Mechanism of Benzyl Alcohol Initiated by OH Radicals: The Addition Channels, ChemPhysChem, 16, 1542-1550, https://doi.org/10.1002/cphc.201500012, 2015.

Wang, S., Zhang, Q., Wang, W., and Wang, Q.: Unexpected enhancement of sulfuric acid-driven new particle formation by alcoholic amines: The role of ion-induced nucleation, J. Environ. Manage., 347, 119079, 10.1016/j.jenvman.2023.119079, 2023.

Wang, X., Jacob, D. J., Eastham, S. D., Sulprizio, M. P., Zhu, L., Chen, Q., Alexander, B., Sherwen, T., Evans, M. J., Lee, B. H., Haskins, J. D., Lopez-Hilfiker, F. D., Thornton, J. A., Huey, G. L., and Liao, H.: The role of chlorine in global tropospheric chemistry, Atmos. Chem. Phys., 19, 3981-4003, 10.5194/acp-19-3981-2019, 2019.

Waterman, R., and Hillhouse, G. L.: η^2 -Organoazide Complexes of Nickel and Their Conversion to Terminal Imido Complexes*via* Dinitrogen Extrusion, J. Am. Chem. Soc., 130, 12628-12629, 10.1021/ja805530z, 2008.

Xie, H., Li, C., He, N., Wang, C., Zhang, S., and Chen, J.: Atmospheric Chemical Reactions of Monoethanolamine Initiated by OH Radical: Mechanistic and Kinetic Study, Environ. Sci. Technol., 48, 1700-1706, 10.1021/es405110t, 2014.

Xie, H., Ma, F., Wang, Y., He, N., Yu, Q., and Chen, J.: Quantum Chemical Study on ·Cl-Initiated Atmospheric Degradation of Monoethanolamine, Environ. Sci. Technol., 49, 13246-13255, 10.1021/acs.est.5b03324, 2015.

Xie, H., Ma, F., Yu, Q., He, N., and Chen, J.: *C*omputational Study of the Reactions of Chlorine Radicals with Atmospheric Organic Compounds Featuring NH_x –π-Bond (x = 1, 2) Structures, J. Phys. Chem. A, 121, 1657-1665, 10.1021/acs.jpca.6b11418, 2017.

Xu, Q., Ma, F., Xia, D., Li, X., Chen, J., Xie, H., and Francisco, J. S.: Two-Step Noncatalyzed Hydrolysis Mechanism of Imines at the Air–Water Interface, J. Am. Chem. Soc., 146, 28866-28873, 10.1021/jacs.4c09080, 2024.

Xue, J., Ma, F., Elm, J., Chen, J., and Xie, H.: Atmospheric oxidation mechanism and kinetics of indole initiated by ·OH and ·Cl: a computational study, Atmos. Chem. Phys., 22, 11543-11555, 10.5194/acp-22-11543-2022, 2022.

Yao, L., Wang, M., Wang, X., Liu, Y., Chen, H., Zheng, J., Nie, W., Ding, A., Geng, F., Wang, D., Chen, J., Worsnop, D. R., and Wang, L.: Detection of atmospheric gaseous amines and amides by a high-

resolution time-of-flight chemical ionization mass spectrometer with protonated ethanol reagent ions, Atmos. Chem. Phys., 16, 14527-14543, 10.5194/acp-16-14527-2016, 2016.

Yi, X., Sarwar, G., Bian, J., Huang, L., Li, Q., Jiang, S., Liu, H., Wang, Y., Chen, H., Wang, T., Chen, J., Saiz Lopez, A., Wong, D. C., and Li, L.: Significant Impact of Reactive Chlorine on Complex Air Pollution Over the Yangtze River Delta Region, China, J GEOPHYS RES-ATMOS, 128, e2023JD038898, 10.1029/2023JD038898, 2023.

Yin, S., Yi, X., Li, L., Huang, L., Ooi, M. C. G., Wang, Y., Allen, D. T., and Streets, D. G.: An Updated Anthropogenic Emission Inventory of Reactive Chlorine Precursors in China, ACS Earth Space Chem., 6, 1846-1857, 10.1021/acsearthspacechem.2c00096, 2022.

You, B., Zhou, W., Li, J., Li, Z., and Sun, Y.: A review of indoor Gaseous organic compounds and human chemical Exposure: Insights from Real-time measurements, Environ. Int., 170, 107611, 10.1016/j.envint.2022.107611, 2022.

Young, C. J., Washenfelder, R. A., Edwards, P. M., Parrish, D. D., Gilman, J. B., Kuster, W. C., Mielke, L. H., Osthoff, H. D., Tsai, C., Pikelnaya, O., Stutz, J., Veres, P. R., Roberts, J. M., Griffith, S., Dusanter, S., Stevens, P. S., Flynn, J., Grossberg, N., Lefer, B., Holloway, J. S., Peischl, J., Ryerson, T. B., Atlas, E. L., Blake, D. R., and Brown, S. S.: Chlorine as a primary radical: evaluation of methods to understand its role in initiation of oxidative cycles, Atmos. Chem. Phys., 14, 3427-3440, 10.5194/acp-14-3427-2014, 2014.

Zhao, Y., and Truhlar, D. G.: The M06 suite of density functionals for main group thermochemistry, thermochemical kinetics, noncovalent interactions, excited states, and transition elements: two new functionals and systematic testing of four M06-class functionals and 12 other functionals, Theor. Chem. Acc., 120, 215-241, 10.1007/s00214-007-0310-x, 2008.

Zhu, S., Yan, C., Zheng, J., Chen, C., Ning, H., Yang, D., Wang, M., Ma, Y., Zhan, J., Hua, C., Yin, R., Li, Y., Liu, Y., Jiang, J., Yao, L., Wang, L., Kulmala, M., and Worsnop, D. R.: Observation and Source Apportionment of Atmospheric Alkaline Gases in Urban Beijing, Environ. Sci. Technol., 56, 17545-17555, 10.1021/acs.est.2c03584, 2022.